JBIC Journal of Biological Inorganic Chemistry (2021) 26:809–815
https://doi.org/10.1007/s00775-021-01897-1

ORIGINAL PAPER

Determining the structure and binding mechanism of oxytocin-Cu^{2+} complex using paramagnetic relaxation enhancement NMR analysis

Israel Alshanski[1] · Deborah E. Shalev[2,3] · Shlomo Yitzchaik[1] · Mattan Hurevich[1]

Received: 5 July 2021 / Accepted: 23 August 2021 / Published online: 30 August 2021

Abstract

Oxytocin is a neuropeptide that binds copper ions in nature. The structure of oxytocin in interaction with Cu^{2+} was determined here by NMR, showing which atoms of the peptide are involved in binding. Paramagnetic relaxation enhancement NMR analyses indicated a binding mechanism where the amino terminus was required for binding and subsequently Tyr2, Ile3 and Gln4 bound in that order. The aromatic ring of Tyr2 formed a π-cation interaction with Cu^{2+}.

Graphic abstract

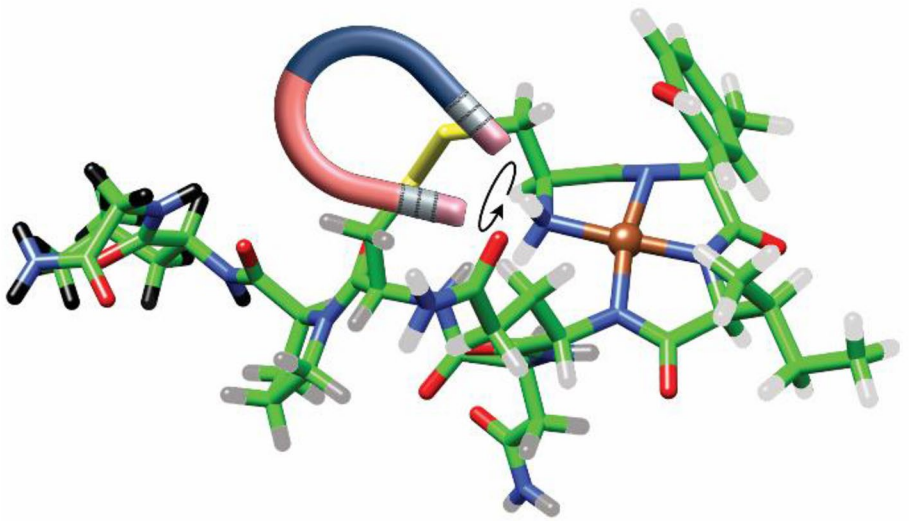

Oxytocin copper complex structure revealed by paramagnetic relaxation enhancement NMR analyses

Keywords Nuclear magnetic resonance · Peptide · Copper complex · Oxytocin · Paramagnetic resonance enhancement

✉ Deborah E. Shalev
debbie.shalev@mail.huji.ac.il

✉ Shlomo Yitzchaik
shlomo.yitzchaik@mail.huji.ac.il

✉ Mattan Hurevich
mattan.hurevich@mail.huji.ac.il
https://scholars.huji.ac.il/mattanhurevich/home

[1] Institute of Chemistry and Center for Nanoscience and Nanotechnology, The Hebrew University of Jerusalem, Edmond J. Safra Campus, Givat Ram, 91904 Jerusalem, Israel

[2] Department of Pharmaceutical Engineering, Azrieli College of Engineering Jerusalem, 91035 Jerusalem, Israel

[3] Wolfson Centre for Applied Structural Biology, The Hebrew University of Jerusalem, Edmond J. Safra Campus, Givat Ram, 91904 Jerusalem, Israel

Introduction

Oxytocin (OT) is a nine-amino acid metal-ion binding cyclic peptide (Fig. 1A) that serves as a neurotransmitter and hormone, and binds the oxytocin G protein-coupled receptor (OTR) [1]. OT is involved in social bonding [2], sexual attraction [3], maternal bonding [3] and childbirth [4]. Copper is an essential metal in nature, but is toxic in its unbound form, hence its binding and transport must be carefully regulated [5, 6]. OT binds copper ions (Cu^{2+}), changing the conformation of the peptide and its affinity to the OTR [7–9].

Copper ions have been shown to bind OT through the terminal amine and several backbone amides which are deprotonated as part of the complexation process. The mechanism of Cu^{2+} binding by OT has been studied by several methods such as affinity chromatography, mass spectroscopy (MS), and electrochemistry [7, 8, 10–17]. An electron paramagnetic resonance (EPR) and potentiometric measurement analysis of OT determined that $[OT\text{-}Cu^{2+}]^-$ is a planar complex in which three amide hydrogens are deprotonated [11, 18]. The EPR study showed that Cys1, Tyr2, Ile3 and Gln4 are the OT amino acids involved in Cu^{2+}-binding (Fig. 1B). Works using electrospray ionization mass spectrometry with collision-induced dissociation (MS-CID), suggested that the $[OT\text{-}Cu^{2+}]^-$ complex was formed via the amide backbone of amino acids Cys1, Cys6, Leu8 and Gly9 (Fig. 1B) [7]. Additional studies that analyzed the $[OT\text{-}Cu^{2+}]^-$ complex by MS-CID suggested yet a different binding mode in which the copper is complexed with either: Tyr2, Ile3, Gln4, and Asn5; Ile3, Gln4, Asn5 and Cys6; or Cys1, Tyr2, Cys6 and a solvent ligand (Fig. 1B) [19, 20]. Many of the above studies were performed in the gas phase after ionization and not in a biologically relevant aqueous solution. Furthermore, the disparity between the complexation modes calls for a more decisive analysis of this crucial interaction.

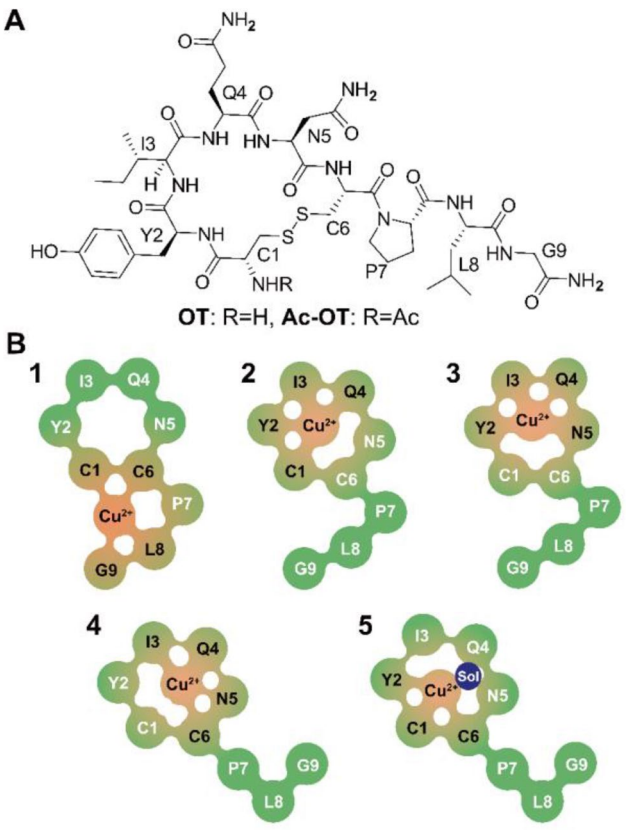

Fig. 1 **a** Schematic structure of OT and Ac-OT. **b** Proposed Cu^{2+} binding moieties in OT based on EPR (2) and by CID-MS (1,3,4,5). Black and white letters indicate copper-bound and unbound amino acids, respectively, as suggested by each model. Solvent ligands are marked in blue

Crystallography and nuclear magnetic resonance (NMR) are the most common methods for determining peptide structures and may provide a way to define the exact amino acids involved in OT-Cu^{2+} complexation [21]. Surprisingly, the exact amino acids involved in OT-Cu^{2+} complexation were never determined by these direct structural methods. The NMR analysis of OT-Cu^{2+} is hindered by the paramagnetic properties and slow relaxation of Cu^{2+}, which results in extreme broadening out of signals of nuclei that are within 8 Å of the Cu^{2+} ion [22, 23].

Many studies show that the effect of metal ion proximity on NMR signals can be utilized for structural analysis [23–25]. For example, lanthanides provide structural information since the shift in NMR signals correlates the distance from the complexed metal ion. Cu^{2+} proximity has shown to be a useful tool for structural analysis [26, 27]. Paramagnetic Cu^{2+} causes extreme line broadening due to the combined effects of paramagnetic relaxation enhancement (PRE) and pseudo contact shifts (PCS) [25, 28–31]. Cu^{2+} is nearly isotropic and has a PRE effect that erases peak signals up to a distance of 8 Å from its nucleus [22, 23, 32, 33]. While erasing peaks in NMR is usually a disadvantage, it can provide information on the proximity of the ion to specific moieties and of the entire complex structure. The PRE and PCS effects of Cu^{2+} have been used to determine protein-ion and fatty acid-ion structures by solution NMR [23, 34].

Solution-state NMR together with PRE information were used to analyze the binding mode and structure of $[OT\text{-}Cu^{2+}]^-$ and to determine which amino acid moieties are involved in $[OT\text{-}Cu^{2+}]^-$ complexation. The binding mechanism of the $[OT\text{-}Cu^{2+}]^-$complex was elucidated based on the PRE response of OT resonances during titration with Cu^{2+}, and the structure was determined while in fast exchange with copper [24, 32].

Results and discussion

We first determined the structure of unbound OT by solution NMR to better evaluate the effect of copper complexation at later stages. The assignment and structure of unbound OT were determined in 5 mM acetate buffer at pH 6.75 to avoid pH-dependent changes in structure or chemical shift due to release of the amide protons upon subsequent Cu^{2+} binding. The ensemble was well-resolved where the low energy ensemble of 14 of the 50 calculated structures had backbone and heavy atom RMSD values of 0.72 and 1.22 Å, respectively (See details in ESI). Half of the low energy conformations were stabilized by a hydrogen bond between the Tyr2 amide proton and the Asn5 carbonyl oxygen (Assignment in Table S1, structures in Figure S3). When this ensemble was compared to a previously solved structure in pure water [35] (PDBid 2MGO) the lowest conformations of each ensemble had a backbone RMSD of 2.10 Å suggesting that the structures were dissimilar under the respective measured conditions.

The ability of OT to bind Cu^{2+} under these conditions was determined by titration. OT was titrated at 20 °C with aliquots of Cu^{2+} to give a 1/20th molar ratio to OT. NMR spectra were recorded after each titration step (Fig. 2). The NMR hydrogen peaks showed changes in chemical shift, in both broadening and a decrease in signal (Fig. 2 and Figure S4). These signal changes indicate binding to Cu^{2+} because:

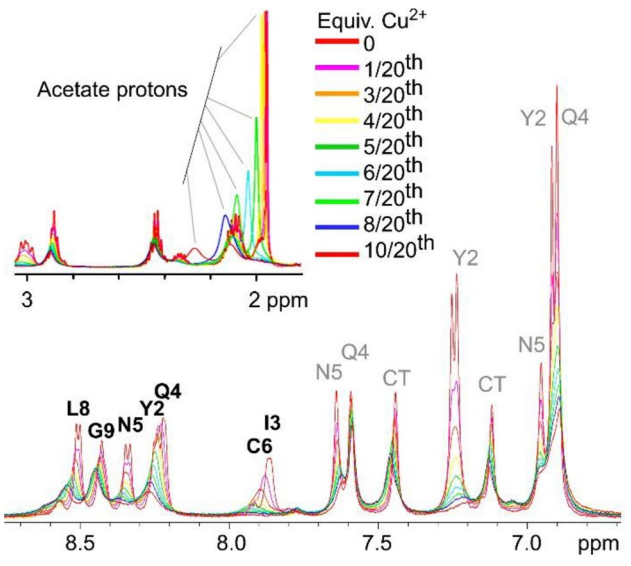

Fig. 2 1D ^{1}H-NMR spectra of OT titration with Cu^{2+} at 20 °C showing chemical shift broadening as a function of Cu^{2+} concentration. Fingerprint region with amide assignment in black and side-chain assignment in grey (CT is C-terminal amidation). Inset shows increasing broadening of the buffer acetate protons as a function of titration

(1) The decrease in signal could stem from deprotonation as part of the Cu^{2+}-binding mechanism; (2) The broadening can be attributed to the paramagnetic effect due to Cu^{2+} proximity; (3) The change in chemical shift may indicate a different chemical environment and/or a change in water exchange rate upon binding.

Several studies have shown that the OT terminal amine plays a key role in Cu^{2+}-binding [11, 17]. An *N*-acetylated OT analog (Ac-OT) was synthesized and studied to determine the effect of blocking the terminal amine on Cu^{2+} binding. Ac-OT was titrated at 20 °C with aliquots of Cu^{2+} to give 1/20th of the molar ratio of the peptide. The NMR spectra (Fig. 3) showed there was no significant change in the intensity of any of the peptide peaks (Fig. 3). The acetate peak from the buffer displayed a marked change in chemical shift and broadened out as a function of the Cu^{2+} concentration, serving as an internal control for Cu^{2+}. Furthermore, the increased degree of broadening of the buffer acetate peak in the Ac-OT titration relative to the OT titration indicated that the copper was not bound by the peptide but complexed the acetate instead. This indicates that Ac-OT does not bind Cu^{2+}, proving that the N-terminus is essential for Cu^{2+} – OT binding.

The detailed mechanism of binding was elucidated by following the Cu^{2+} titration of OT by 2D NMR. The TOCSY spectrum at 20 °C (Fig. 4) showed resolved peaks (Fig. 4A). The degree of change in chemical shift and reduction in signal due to broadening out with increasing Cu^{2+} concentration was determined for each hydrogen in the peptide (e.g., Fig. 4B). The HN signal of Ile3 disappeared upon adding the first aliquot of Cu^{2+} and the HN signal of Tyr2 was not

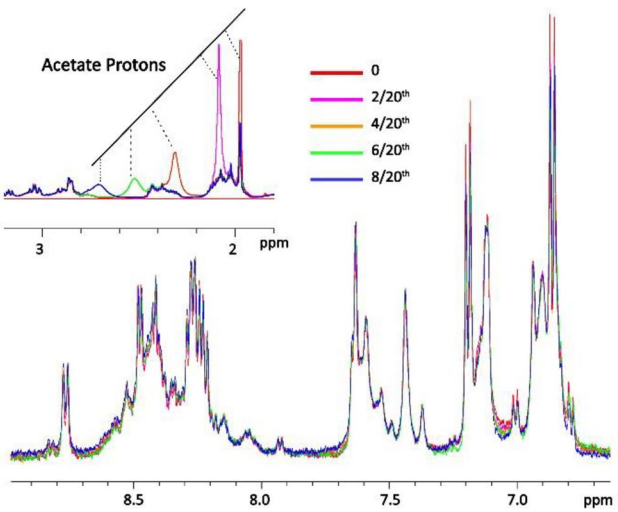

Fig. 3 1D ^{1}H-NMR spectrum of N-acetylated OT titration with Cu^{2+} at 20 °C showing no effect of the Cu^{2+} on the chemical shift or broadening of OT, but broadening of the acetate buffer signal as a function of Cu^{2+} concentration. The intensities of the spectra are corrected for dilution

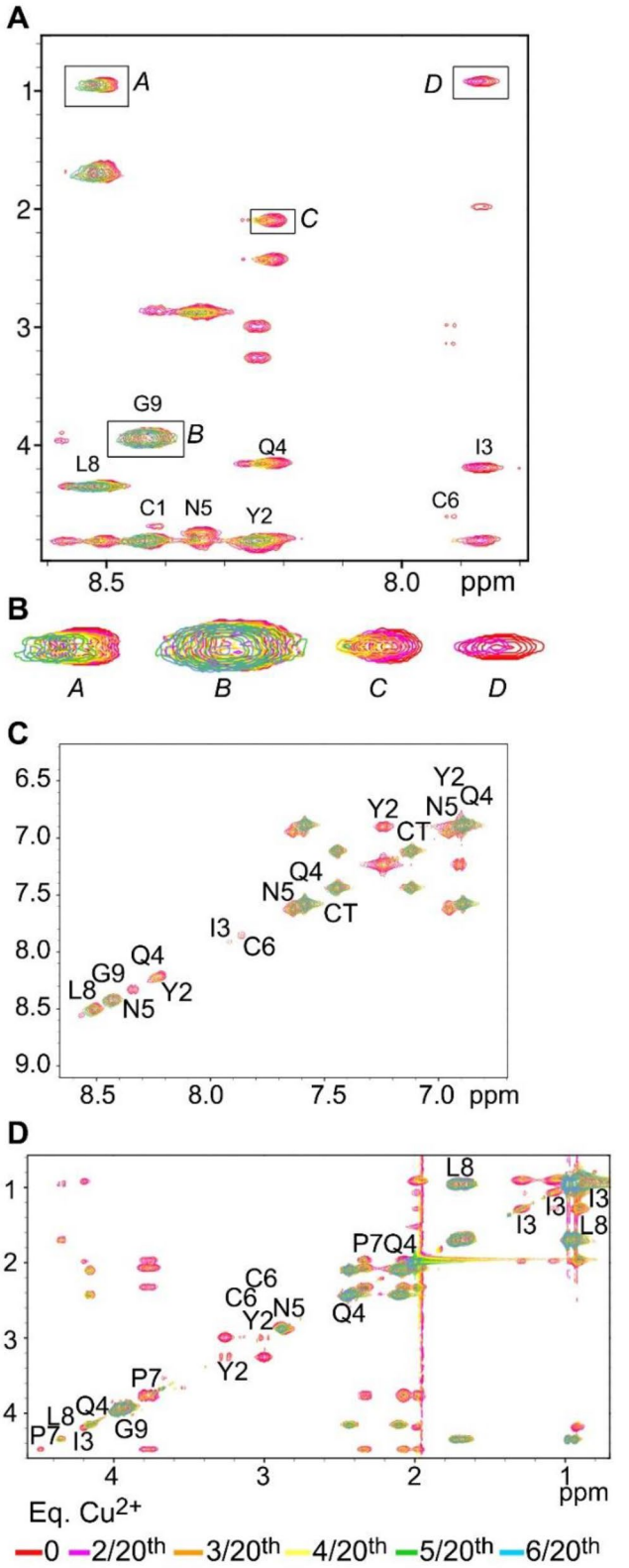

Fig. 4 2D ^{1}H-NMR TOCSY spectra of OT titration with Cu^{2+} at 20 °C showing **a** fingerprint region; **b** enlarged peaks from fingerprint region to exemplify broadening out (e.g., *C* and *D*) and chemical shift changes (e.g., *A*, *C* and *D*) and as a function of Cu^{2+} concentration; **c** the backbone and sidechain amide and aromatic regions and **d** aliphatic region of the TOCSY spectra

evident in the spectrum after 3/20th molar equivalents of Cu^{2+} (Fig. 4C). The HN of Gln4 was lost after 5/20th and that of Asn5 was still barely evident at the end of the titration. Amide signals of Cys1 and Cys6 had low intensity in the non-titrated spectrum and could not be used for mechanistic study. The HN signal of Leu8 showed significant change in chemical shift (Fig. 4B peak *A*), but neither it nor Gly9 HN completely broadened out. Throughout the titration, the Gln4 and Asn5 sidechain amide, and C-terminus amidation resonances were evident, whereas, Tyr2 aromatic signals disappeared after 4/20th molar equivalents of Cu^{2+}. Non-exchangeable hydrogens in the aliphatic region of the spectrum (Fig. 4D) also disappeared due to close proximity to Cu^{2+}, including Tyr2 α and β hydrogens that disappeared at the 3/20th aliquot, Ile3 and Pro7 at the 4/20th aliquot and Gln4 at the 5/20th aliquot, Asn5 was significantly reduced but still evident at the end of the titration, and Leu8 and Gly9 persisted throughout the titration. Stronger binding was seen in the parallel titration of OT with Cu^{2+} at 14 °C, as expected, and the spectral phenomena were the same (Figure S5).

Hydrogens which were further away showed changes in chemical shift owing to the structural changes in the peptides that resulted from Cu^{2+}-binding. Together, the results suggested a binding mode where the N-terminus nitrogen was both the first to bind and was a prerequisite for binding since there was no broadening when the Cys1 amine was acetylated (Fig. 3). Subsequently Tyr2, then Ile3 and finally Gln4 probably bind in that order, as that is the order of reduction of amide signal. The sidechains of Tyr2 and Ile3 were strongly affected by the paramagnetic broadening, indicating a close proximity to the Cu^{2+}. The changes in chemical shift of Leu8 and Gly9 were probably due to changes in equilibrium structure due to binding.

Spectral analysis indicated the binding sequence. Since binding Cu^{2+} necessarily exchanges the backbone amide, the order of which the backbone amide signal was lost presumably indicated the order by which the amino acids bind Cu^{2+}. Amino acids within 8 Å of the Cu^{2+} ion were paramagnetically broadened out.

The identities of the amino acids that bound Cu^{2+} were used together with the NMR-derived NOE distance restraints to solve the structure of the $[OT\text{-}Cu^{2+}]^{-}$ complex at 20 °C while in equilibrium between a bound and free form. Structural COSY [36], TOCSY [37], using the MLEV-17 pulse scheme for the spin lock (150 ms) [36], and rotating frame overhauser effect spectroscopy (ROESY) experiments[36, 38, 39] were acquired under identical conditions (see Supplementary information), assigned [40] (Figure S6 and Table S1) and the NOE restraints were derived in the presence of 1/10th of a molar equivalent of Cu^{2+} to OT. The ROESY spectrum gave a total of 78 NOE interactions, comprising 54 intraresidual, 20 sequential and 4 longer range

interactions. As stated, the signals for Cys1 and Cys6 had extremely low intensity in both the unbound OT and when in complex with Cu^{2+} and did not provide any structural information of the region. The structure was determined using XPLOR-NIH [41, 42] where covalent bonds to Cu^{2+} were introduced for the four determined ligand nitrogens, Cys1, Tyr2, Ile3 and Gln4 using known square planar geometry [11, 43]. The resulting ensemble of 50 structures had no violations of canonical geometry and backbone and heavy atom RMSD values of 1.29 and 2.28 Å, respectively. The 16 lowest energy conformations showed a stable structure with RMSD values of 0.80 and 1.38 Å, respectively. The presented 10 low energy structures (Fig. 5) had overall backbone and heavy atom RMSD values of 0.60 and 1.21 Å, respectively, and RMSD values in the OT ring region of residues 1–6 of 0.10 and 0.94 Å, respectively.

The conformation was compared to that of unbound OT to ensure that we were not measuring the free fraction of the sample (Figure S6). The free structure was compared to the bound structure without constraints to the Cu^{2+} to ascertain that the NOE constraints led to a new structure and that the bound Cu^{2+} was not inducing all the structural changes (Figure S6). The RMSD of the ring residues 1–6 of OT in the lowest calculated structures of the unbound molecule to those of the OT-Cu^{2+} complex without introducing the Cu^{2+} bonds, was 2.19 Å, which is much larger than each individual RMSD (above and in Supplementary Information), strongly indicating that the structures are distinct.

The low-energy ensemble of the $[OT\text{-}Cu^{2+}]^{-}$ complex (Fig. 5; PDBid 7OTD) shows a rigid ring area binding the Cu^{2+} and the Tyr2 aromatic ring within 3.5–5.8 Å of the metal ion center as has been seen in other systems [44–47]. The hydrogens that disappeared at the initial stage of the titration were within 5 Å of the Cu^{2+} explaining their early broadening out, and amino acids 1–7, which showed significant deviation of chemical shift upon titration, all resided within 8 Å of the Cu^{2+} in purple (Fig. 5). Asn 5 is above the plane of the bound copper with α, β and δ sidechain hydrogens at an average of 4.0, 5.5 and 7.9 Å, respectively. Leu8 and Gly9 are farther from the paramagnetic center and show changes in chemical shift associated with structural changes in OT upon binding.

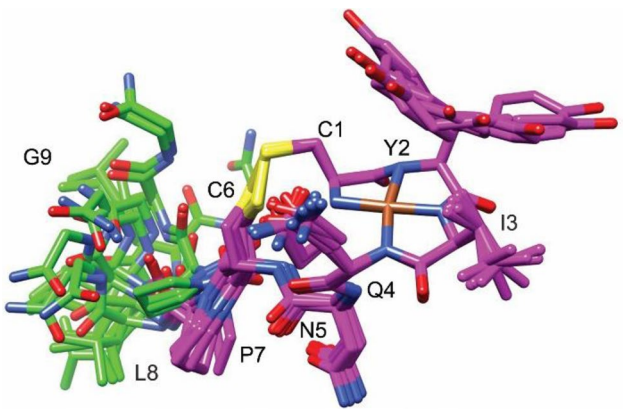

Fig. 5 Low energy conformational space of OT-Cu^{2+} complex at 20 °C, showing atoms within 8 Å of the Cu^{2+} in purple

This structure has a loss of resolution in the Cys–Cys bond region since the NMR signal is faint even in the non-bound spectrum before titration. Nonetheless, the titration analysis strongly correlates the structural results of the non-exchangeable hydrogens. Our proposed Cu^{2+}-binding amino acids agree with the one reported by Bal et al. utilizing EPR [11]. Other reports, which utilized MS-CID, suggest different binding modes of OT [7, 13, 14, 19]. The variation between the models stem from differences in methodologies but may also hint at intricacies of Cu^{2+} transport by the peptide, which leads to several complexation modes.

Conclusion

This is the first time that the complex between OT and copper was determined in solution using NMR analysis. PRE of OT upon titration with Cu^{2+} was measured by NMR and used to map the binding amino acids that serve as copper ligands under these solution conditions and indicated the order of attachment during the binding process. The titration of OT and Ac-OT solutions with Cu^{2+} resulted in the following findings: (i) OT binding required the free Cys1 amino terminus for binding. (ii) Tyr2, Ile3 and Gln4 subsequently bound to the Cu^{2+} ion in that order. (iii) The conformational space of the [OT-Cu^{2+}] complex showed the aromatic sidechain of Tyr2 within range of the Cu^{2+} to undergo a π-cation interaction. These findings give insight into the way copper binds OT in aqueous buffered media and hence may reflect on the nature of this important complex in the physiological environment. Therefore, peptidomimetics can be designed based on this structure and NMR can be used to study important complexes of small peptides with paramagnetic metal ions.

Supplementary Information The online version contains supplementary material available at https://doi.org/10.1007/s00775-021-01897-1.

Acknowledgements The authors would like to thank RECORD-IT project. This project has received funding from the European Union's Horizon 2020 research and innovation programme under grant agreement No 664786; SY is the Benjamin H. Birstein Chair in Chemistry. IA is supported by a Hebrew University Center for Nanoscience and Nanotechnology Ph.D. scholarship.

Declarations

Conflict of interest The authors have no conflicts of interest to declare.

References

1. Arrowsmith S (2020) Oxytocin and vasopressin signalling and myometrial contraction. Curr Opin Physiol 13:62–70. https://doi.org/10.1016/j.cophys.2019.10.006
2. Insel TR (2010) The challenge of translation in social neuroscience: a review of oxytocin, vasopressin, and affiliative behavior. Neuron 65:768–779. https://doi.org/10.1016/j.neuron.2010.03.005
3. Kendrick KM (2005) Oxytocin, motherhood and bonding. Exp Physiol 85:111s–124s. https://doi.org/10.1136/bmj.2.3798.755-b
4. Knobloch HS, Charlet A, Hoffmann LC et al (2012) Evoked axonal oxytocin release in the central amygdala attenuates fear response. Neuron 73:553–566. https://doi.org/10.1016/j.neuron.2011.11.030
5. Rubino JT, Franz KJ (2012) Coordination chemistry of copper proteins: how nature handles a toxic cargo for essential function. J Inorg Biochem 107:129–143. https://doi.org/10.1016/j.jinorgbio.2011.11.024
6. Shanbhag VC, Gudekar N, Jasmer K et al (2021) Copper metabolism as a unique vulnerability in cancer. Biochim Biophys Acta Mol Cell Res 1868:118893. https://doi.org/10.1016/j.bbamcr.2020.118893
7. Wyttenbach T, Liu D, Bowers MT (2008) Interaction of divalent metal ions with the hormone oxytocin: hormone receptor binding. J Am Chem Soc 130:1–19. https://doi.org/10.1021/ja8002342
8. Liu D, Seuthe AB, Ehrler OT et al (2005) Oxytocin-receptor binding: why divalent metals are essential. J Am Chem Soc 127:2024–2025. https://doi.org/10.1021/ja046042v
9. Pearlmutter AF, Soloff MS (1979) Characterization of the metal ion requirement for oxytocin-receptor interaction in rat mammary gland membranes. J Biol Chem 254:3899–3906
10. Bal W, Dyba M, Kozłowski H (1997) The impact of the amino-acid sequence on the specificity of Copper(II) interactions with peptides having nonco-ordinating side-chains. Acta Biochim Pol 44:467–476
11. Bal W, Kozlowski H, Lammek B et al (1992) Potentiometric and spectroscopic studies of the Cu(II) complexes of Ala-Arg8-vasopressin and oxytocin: two vasopressin-like peptides. J Inorg Biochem 45:193–202. https://doi.org/10.1016/0162-0134(92)80044-V
12. Tadi KK, Alshanski I, Mervinetsky E et al (2017) Oxytocin-monolayer-based impedimetric biosensor for zinc and copper ions. ACS Omega 2:8770–8778. https://doi.org/10.1021/acsomega.7b01404
13. Joly L, Antoine R, Albrieux F et al (2009) Optical and structural properties of copper-oxytocin dications in the gas phase. J Phys Chem B 113:11293–11300. https://doi.org/10.1021/jp9037478
14. Joly L, Antoine R, Allouche AR et al (2009) Optical properties of isolated hormone oxytocin dianions: ionization, reduction, and copper complexation effects. J Phys Chem A 113:6607–6611. https://doi.org/10.1021/jp810342s
15. Peter D, Varnagy K, Sovago I et al (1995) Potentiometric and spectroscopic studies on the Copper(II) complexes of peptide hormones containing disulfide bridges. J Inorg Biochem 60:69–78. https://doi.org/10.1016/S0020-1693(98)00079-6
16. Mervinetsky E, Alshanski I, Buchwald J et al (2019) Direct assembly and metal ions binding properties of oxytocin monolayer on gold surfaces. Langmuir 35:11114–11122. https://doi.org/10.1021/acs.langmuir.9b01830
17. Mervinetsky E, Alshanski I, Tadi KK et al (2020) A zinc selective oxytocin based biosensor. J Mater Chem B 8:155–160. https://doi.org/10.1039/c9tb01932d
18. Blount FJ, Freeman HC, Holland VR, Milburn WHG (1970) Crystallographic studies of metal-peptide complexes. J Biol Chem Chem 245:5177–5185
19. Jayasekharan T, Gupta SL, Dhiman V (2018) Binding of Cu+ and Cu2+ with peptides: peptides = oxytocin, Arg8-vasopressin, bradykinin, angiotensin-I, substance-P, somatostatin, and neurotensin. J Mass Spectrom 53:296–313. https://doi.org/10.1002/jms.4062
20. Jeong HJ, Kim HT (2009) Determination of a binding site of Cu and Ni metal ions with oxytocin peptide by electrospray tandem mass spectrometry and multiple mass spectrometry. Eur J Mass Spectrom 15:67–72. https://doi.org/10.1255/ejms.977
21. Dyson HJ, Wright PE (1991) Defining solution conformations of small linear peptides. Annu Rev Biophys Biophys Chem 20:519–538. https://doi.org/10.1146/annurev.bb.20.060191.002511
22. Ubbink M, Lian LY, Modi S et al (1996) Analysis of the 1H-NMR chemical shifts of Cu(I)-, Cu(II)- and Cd-substituted pea plastocyanin. Metal-dependent differences in the hydrogen-bond network around the copper site. Eur J Biochem 242:132–147. https://doi.org/10.1111/j.1432-1033.1996.0132r.x
23. Ubbink M, Worrall JAR, Canters GW et al (2002) Paramagnetic resonance of biological metal centers. Annu Rev Biophys Biomol Struct 31:393–422. https://doi.org/10.1146/annurev.biophys.31.091701.171000
24. Pintacuda G, John M, Su XC, Otting G (2007) NMR structure determination of protein—ligand complexes by lanthanide labeling. Acc Chem Res 40:206–212. https://doi.org/10.1021/ar050087z
25. Otting G (2010) Protein NMR using paramagnetic ions. Annu Rev Biophys 39:387–405. https://doi.org/10.1146/annurev.biophys.093008.131321
26. Bertini I, Ciurli S, Dikiy A et al (2001) The first solution structure of a paramagnetic Copper(II) protein: the case of oxidized plastocyanin from the cyanobacterium synechocystis PCC6803. J Am Chem Soc 123:2405–2413. https://doi.org/10.1021/ja0033685
27. Brandt M, Gammeltoft S, Jensen KJ (2006) Microwave heating for solid-phase peptide synthesis: general evaluation and application to 15-mer phosphopeptides. Int J Pept Res Ther 12:349–357. https://doi.org/10.1007/s10989-006-9038-z
28. Arnesano F, Banci L, Bertini I et al (2003) A strategy for the NMR characterization of type II Copper(II) proteins: the case of the copper trafficking protein CopC from Pseudomonas syringae. J Am Chem Soc 125:7200–7208. https://doi.org/10.1021/ja034112c
29. John M, Otting G (2007) Strategies for measurements of pseudocontact shifts in protein NMR spectroscopy. ChemPhysChem 8:2309–2313. https://doi.org/10.1002/cphc.200700510
30. Cerofolini L, Silva JM, Ravera E et al (2019) How do nuclei couple to the magnetic moment of a paramagnetic center? A new theory at the gauntlet of the experiments. J Phys Chem Lett 10:3610–3614. https://doi.org/10.1021/acs.jpclett.9b01128
31. Bertini I, Felli IC, Luchinat C et al (2007) Towards a protocol for solution structure determination of copper(II) proteins: the case of CuIIZnII superoxide dismutase. ChemBioChem 8:1422–1429. https://doi.org/10.1002/cbic.200700006
32. Banci L, Pierattelli R, Vila AJ (2002) Nuclear magnetic resonance spectroscopy studies on copper proteins. Adv Protein Chem 60:397–406. https://doi.org/10.1016/S0065-3233(02)60058-0
33. Milardi D, Arnesano F, Grasso G et al (2007) Ubiquitin stability and the Lys 63-linked polyubiquitination site are compromised on copper binding. Angew Chemie 119:8139–8141. https://doi.org/10.1002/ange.200701987
34. Wuthrich K (2001) Nuclear magnetic resonance spectroscopy of proteins. eLS. https://doi.org/10.1038/npg.els.0003103
35. Koehbach J, O'Brien M, Muttenthaler M et al (2013) Oxytocic plant cyclotides as templates for peptide G protein-coupled receptor ligand design. Proc Natl Acad Sci USA 110:21183–21188. https://doi.org/10.1073/pnas.1311183110

36. Aue WP, Bartholdi E, Ernst RR (1976) Two-dimensional spectroscopy. Application to nuclear magnetic resonance. J Chem Phys 64:2229–2246. https://doi.org/10.1063/1.432450
37. Bax AD, Donald GD (1985) MLEV-17-based two-dimensional homonuclear magnetization transfer spectroscopy. J Magn Reson 65:355–360
38. Piotto M, Sau DV, Sklenar V (1992) Tap or bottled water gradient-tailored excitation for single-quantum NMR spectroscopy of aqueous solutions. J Biomol NMR 2:661–665
39. Sklenář V, Piotto M, Leppik R, Saudek V (1993) Gradient-tailored water suppression for 1H–15N HSQC experiments optimized to retain full sensitivity. J Magn Reson Ser A 102:241–245
40. Wüthrich K (1986) NMR with proteins and nucleic acids. Wiley, USA
41. Schwieters CD, Kuszewski JJ, Tjandra N, Clore GM (2003) The Xplor-NIH NMR molecular structure determination package. J Magn Reson 160:65–73. https://doi.org/10.1016/S1090-7807(02)00014-9
42. Schwieters CD, Kuszewski JJ, Marius Clore G (2006) Using Xplor-NIH for NMR molecular structure determination. Prog Nucl Magn Reson Spectrosc 48:47–62. https://doi.org/10.1016/j.pnmrs.2005.10.001
43. Blount JF, Freeman HC, Holland RV, Milburn GHW (1970) Crystallographic studies of metal-peptide complexes. J Biol Chem 245:5177–5185. https://doi.org/10.1016/s0021-9258(18)62739-5
44. Sugimori T, Shibakawa K, Masuda H et al (1993) Ternary Metal(II) complexes with tyrosine-containing dipeptides. Structures of Copper(II) and Palladium(II) complexes involving L-Tyrosylglycine and stabilization of Copper(II) Complexes due to intramolecular aromatic ring stacking. Inorg Chem 32:4951–4959. https://doi.org/10.1021/ic00074a047
45. Abdelhamid RF, Obara Y, Uchida Y et al (2007) π-π interaction between aromatic ring and copper-coordinated His81 imidazole regulates the blue copper active-site structure. J Biol Inorg Chem 12:165–173. https://doi.org/10.1007/s00775-006-0176-8
46. Ito N, Phillips SEV, Stevens C et al (1991) Novel thioether bond revealed by a 1.7 Å crystal structure of galactose oxidase. Nature 350:87–90. https://doi.org/10.1038/350087a0
47. Yajima T, Takamido R, Shimazaki Y et al (2007) π-π Stacking assisted binding of aromatic amino acids by Copper(II)-aromatic diimine complexes. Effects of ring substituents on ternary complex stability. Dalt Trans. https://doi.org/10.1039/b612394e